

DRIVEN PIPE PILES IN DENSE SAND

BYRON BYRNE

**GEOMECHANICS GROUP
THE UNIVERSITY OF WESTERN AUSTRALIA**

ABSTRACT: Piles are often driven open ended into dense sand with the aim of increasing the ease of penetration of the pile. Generally, the pile tip contains an internal driving shoe in order to allow soil to enter the pile, forming a soil plug. The type of shoe influences the length of the soil plug and the ease of penetration of the pile. The paper describes the results of field tests undertaken on a 2.2 m long, by 51 mm diameter, pile, fitted with five different driving shoes and driven into dense sand. Dynamic and static load tests showed good correlations between the type of driving shoe, plug formation rate, and eventual end bearing capacity. It was found that the dynamic measurements provided a lower bound estimate of axial capacity. The measured capacities were significantly higher than those estimated from current design codes.

1. INTRODUCTION

Piles are driven open ended to increase the ease of penetration, particularly when dense sand layers exist in the soil stratigraphy. This enables the pile to be installed to the full design length and thus the design capacity of the pile to be obtained. This is especially relevant to long piles which are often designed for friction, with the end bearing component making little contribution to the final capacity. In this mode of penetration a plug of soil forms up the middle of the pile. This project looks to enhance the knowledge base that exists (eg Bruzy et al, 1991), on how this soil plug affects the performance of the pile, by analysing a number of field tests that include both open and closed ended piles. Specifically, the aim of the research was to investigate:

- a) How different driving shoes affected the penetration of the soil into the pile, and the required driving energy.
- b) How the 'plugging ratio' (incremental ratio of length of soil plug to penetration of pile) affected the shaft and end bearing resistance of the pile.
- c) The accuracy of dynamic measurements of soil resistance for predicting the tensile and compressive capacity of driven piles.

2. OVERVIEW

A total of 15 field tests were performed at a site in Shenton Park, encompassing dynamic and static tests on a steel pipe pile driven into dense sand, using five different driving shoes. Further data were gathered from a previous thesis (Kain, 1993) which looked at 6 tests also performed at the same site. All 21 sets of data were subjected to extensive numerical and comparative analysis.

3. APPARATUS AND PROCEDURE

The 2.2 m long pile was instrumented 200 mm below the pile head in order to take measurements of the transient force and velocity waves during the driving of the pile. The pile outside diameter was 51.1 mm with a wall thickness of 1.6 mm and a variety of shoes were manufactured so as to produce different rates of plugging (see Figure 1). In addition to the extreme cases of (a) closed ended (solid shoe), (b) flush pile

(no shoe), three different driving shoes were explored with the aim of maximising penetration of the soil plug into the pile. The shoes doubled the wall-thickness of the pile at the tip, and extended up to one radius up the inside of the pile allowing the soil to dilate and move easily up the pile once past the sleeve. Once driven to the final embedment, static load tests were performed so that an accurate measure of the pile capacity (both compressive and tensile) could be obtained.

3.1 Design Calculations

The soil consisted of a dense sand with a cone profile as shown in Figure 2. From this profile an estimate of the pile capacity may be obtained using appropriate averaging formulas for both tip (Fleming et al, 1992) and skin friction resistances.

$$Q_s = \pi d l \bar{f}_s = (\pi)(0.0511)(1.7)(19.31) = 5.3 \text{ kN}$$

$$Q_b = A_b q_c = (0.002051)(38125) = 7.82 \text{ kN}$$

$$Q_t = Q_b + Q_s = 5.3 + 7.82 = 13.1 \text{ kN}$$

An alternative approach is to adopt the design code (Fleming et al, 1992) to determine pile capacities. Given that $\tau_s = K \sigma'_v \tan \delta$ and assuming that $K = 1.2$, $\delta = 27^\circ$ and $\gamma = 17 \text{ kN/m}^3$ then $\tau_s = 10.4z \text{ kPa}$ (where z is the depth in m). Also $q_b = N_q \sigma'_v = (40)(17)(1.7) = 1156 \text{ kPa}$ where $N_q = 40$ for $\phi = 30^\circ$. The design estimate of the pile capacity is therefore $Q_s = 2.4 \text{ kN}$ and $Q_b = 2.4 \text{ kN}$ and thus $Q_t = 4.8 \text{ kN}$.

These two approaches vary significantly, with the design code end bearing pressure being a factor of 3 less than that actually mobilised by the cone penetrometer. As well, the design skin friction is a very conservative estimate of the friction profile mobilised in the CPT.

3.2 Dynamic Testing

The pile was driven into the ground by means of a 4 kg drop weight suspended from an aluminium tripod. At pile penetration intervals of 100 mm throughout the installation measurements were taken consisting of pile penetration, plug penetration, and blow count. A drop height of 1 m was generally used for ease of driving. Eight dynamic tests were performed at each of the embedment levels of 600 mm, 1200 mm, and 1700 mm. The dynamic tests were further divided into four having a drop height of 0.5 m and four having a drop height of 1 m. An example stress wave for pile BO6 is shown in Figure 3 at a penetration of 1700 mm with a drop height of 0.5 m. It can be seen that both the force and velocity curves coincide until the soil resistance is encountered (and upward waves are reflected); they then diverge for a full shaft resistance of approximately 5.5 kN. Under dynamic loading the pile fails in an unplugged fashion and this shaft resistance represents the full mobilisation of both internal and external skin friction. The end bearing resistance is fully mobilised as illustrated by the large reflection of the velocity wave from the base of the pile and a permanent set of 2.5 mm. A dynamic capacity maybe calculated from the stress waves by solving the wave equation, which considers the pile as an elastic bar and assumes only axial motion. The total dynamic capacity of 8.4 kN, may be modified by a parameter, j_c , to produce an estimate of the static capacity, known as the Case capacity (Rausche et al, 1985). The soil parameter j_c is obtained from tables or from

previous static load tests performed at the site. For pile BO6 the Case estimate of static capacity is 6.0 kN reached by assuming $j_c = 0.1$, which is appropriate for the site.

3.3 Static Testing

Static load tests in both compression and tension were performed by steadily jacking the pile into the ground (or out of it) and recording load and displacement data points. A typical load settlement curve is shown in Figure 4 for pile BO6. It may be noted from this Figure, that the two strain gauges on either side of the pile lead to different estimates of force. This is due to bending effects which are present for both dynamic and static tests. The actual force is obtained by averaging the two sets of data.

There are various methods of determining the ultimate capacity from these plots, especially in compression. A common method takes Q_{static} as the load required to displace the pile 1/10 of its diameter. Whitaker (1976) suggests that this definition may be applied to the results of a constant penetration rate test, and probably represents a lower limit to the penetration required to develop the full end resistance. For the small pile of diameter 0.0511 m the minimum displacement required is 5.1 mm. Subsequently this method produces a lower bound capacity of about 7.3 kN in compression for pile BO6. The tensile capacity on the other hand is easier to deduce as only external shaft friction is mobilised under failure. This should be fully mobilised by the displacement of 5.1 mm and thus an estimate of tensile capacity for this particular test is 3.1 kN.

3.4 Numerical Analysis

The dynamic data have been analysed using the Impact program (Randolph, 1992) where soil parameters are varied until a match between measured and numerically derived stress waves is obtained. A typical match is shown for pile BO6 in Figure 5. A summary of soil parameters deduced from the stress-wave match shown in Figure 5 is tabulated in Figure 6. It should be noted that these parameters are somewhat operator dependent! It can be seen that the external shaft friction is 3.82 kN whereas the tensile capacity was only 3.1 kN. It has been shown that in non cohesive, free draining soils (such as the sand encountered at Shenton Park) the shaft capacity derived under tensile loading, Q , is significantly lower than under compressive loading Q_c (De Nicola and Randolph, 1993). Reasons for this difference in shaft capacities include Poisson's ratio effect and the change in the total stress field due to the direction of loading. Assuming an interface friction angle $\delta = 27^\circ$ the expression derived by De Nicola and Randolph produces a ratio Q/Q_c of 0.87. The results from Impact suggest the ratio is of the order 0.81 but it should be remembered that the division between shaft and base capacity deduced from the Impact program is operator dependent.

From the Impact output an estimate of pile capacity can be obtained. In all tests undertaken the pile was shown to fail in a fully plugged fashion under static loading; therefore the estimated pile capacity from the dynamic measurements for pile BO6 is 7.45 kN which compares well to the measured static value. Interestingly, a simple driving formula approach (Whitaker, 1976), equating input energy to work done (E

= $R(s + c/2)$ where E is the measured energy, R is the pile resistance, s is the permanent set and c is the temporary compression) leads to $R = 7.32$ kN. This compares closely to the Impact estimates of pile capacity and the measured static load.

4. RESULTS

4.1 Plug Penetration

A range of plugging was achieved by the use of the various sleeved endings as shown in Figure 7. As expected the sleeves produced larger lengths of plug than the plain open ended piles. Although 15 tests were undertaken, the plug penetration data for the common end conditions were averaged and produced remarkably distinct trends between each condition. These trends emerged after the pile had penetrated 400 mm, before which they all appeared to be totally coring (unplugged). It can be seen that the longer sleeves produced larger plug lengths which can be attributed to the larger stress release experienced by the soil once past the sleeve. The sleeved endings produced lower blow counts than the plain open ended piles.

4.2 End Bearing Pressure

The sleeved endings enabled more soil to enter the pile and less soil to be forced out and around the pile tip, thus leading to lower stresses than for the case of flush open-ended piles. Conversely the closed ended pile prevented any soil entering, pushing all soil out and around the pile tip, thus creating a higher stress state at the pile tip. This translates into higher end bearing pressures being developed for the closed ended piles than for the open ended piles (see Figure 8). It can also be noticed that the end bearing pressure mobilised by the closed ended pile does not approach that mobilised by the cone penetrometer ($q_c \sim 3.8$ MPa).

4.3 Blow Rate and Capacity

Figure 9 shows that the blow rate is an extremely good predictor of the capacity of the pile. A driving formula estimate of capacity compares well with the blow rate estimates of capacity (close to a line of best fit). The permanent set in this case is simply the inverse of the blow rate and the other variables can be obtained from an Impact analysis. Figure 9 also shows that higher capacities were measured from tests conducted in the summer than in the winter. In fact some capacities are a factor of two greater. This probably can be attributed to slight cementation between particles in the summer when the moisture content is virtually zero. In the winter this cementation is reduced as the moisture content increases to 7%.

4.4 Predictions from Dynamic Measurements

Dynamic analysis for estimation of capacity is much cheaper than static loading for full scale piles. It is therefore essential to compare dynamic predictions to static measurements (Figure 10). At low capacities the predictions of the axial capacity from the dynamic measurements matches the actual capacities extremely well. These dynamic estimates include the Case analysis, which is a quick estimate of the capacity done on-site, and the subsequent Impact analysis which requires a more time consuming process. At higher capacities the dynamic predictions provide a lower bound.

5. CONCLUSIONS

A number of field tests were undertaken on small pipe piles driven into dense sand. The piles incorporated a variety of pile tip conditions, varying from closed ended, to open ended and three different types of internal sleeve. The sleeves led to improved drivability, with more soil entering the pile to form a soil plug. However it was also found that the final end bearing capacity of the pile decreased linearly with increasing plugging ratio. Tests conducted in the summer months showed higher capacities than tests in the winter months, but in both cases the measured capacity was significantly higher than estimated using current design codes. At the other extreme, estimation of pile capacity directly from the measured cone data overestimated the pile capacity by 30 - 60 %.

Dynamic test results were analysed to give estimates of shaft and base resistance. These estimates agreed reasonably well with the measured capacities in tension and compression. In general, particularly for the higher capacities measured in the summer, the dynamic estimate of pile capacity formed a lower bound to the measured static capacities.

6. REFERENCES

- Brucy, F., Meunier, J. and Nauroy, J-F. (1991), 'Behaviour of pile plug in sandy soils during and after driving', Proc. 23rd An. Offshore Tech. Conference, Houston, OTC 6514, pp. 145 - 154.
- De Nicola, A. and Randolph, M.F. (1993), 'Tensile and compressive shaft capacity of piles in sand', Research report No. G1057, Geomechanics Group, UWA.
- Fleming W.G.K., Weltman A.J., Randolph M.F. and Elson W.K. (1992), 'Piling engineering', Blackie (Halstead Press), 2nd Edition.
- Kain D. (1993), 'Static and dynamic performance of piles', Honours Thesis, University of Western Australia.
- Randolph, M. F. (1992), 'IMPACT - Manual', Geomechanics Group, UWA.
- Rausche F., Goble, G. G. and Likins, G. E. (1985), 'Dynamic determination of pile capacity', J. Geot. Eng. Div., ASCE, 111, 367 - 383.
- Whitaker, T. 1976. 'The design of piled foundations', Pergamon Press, Oxford. pp 26 - 43, 150 - 155. 2nd Edition.

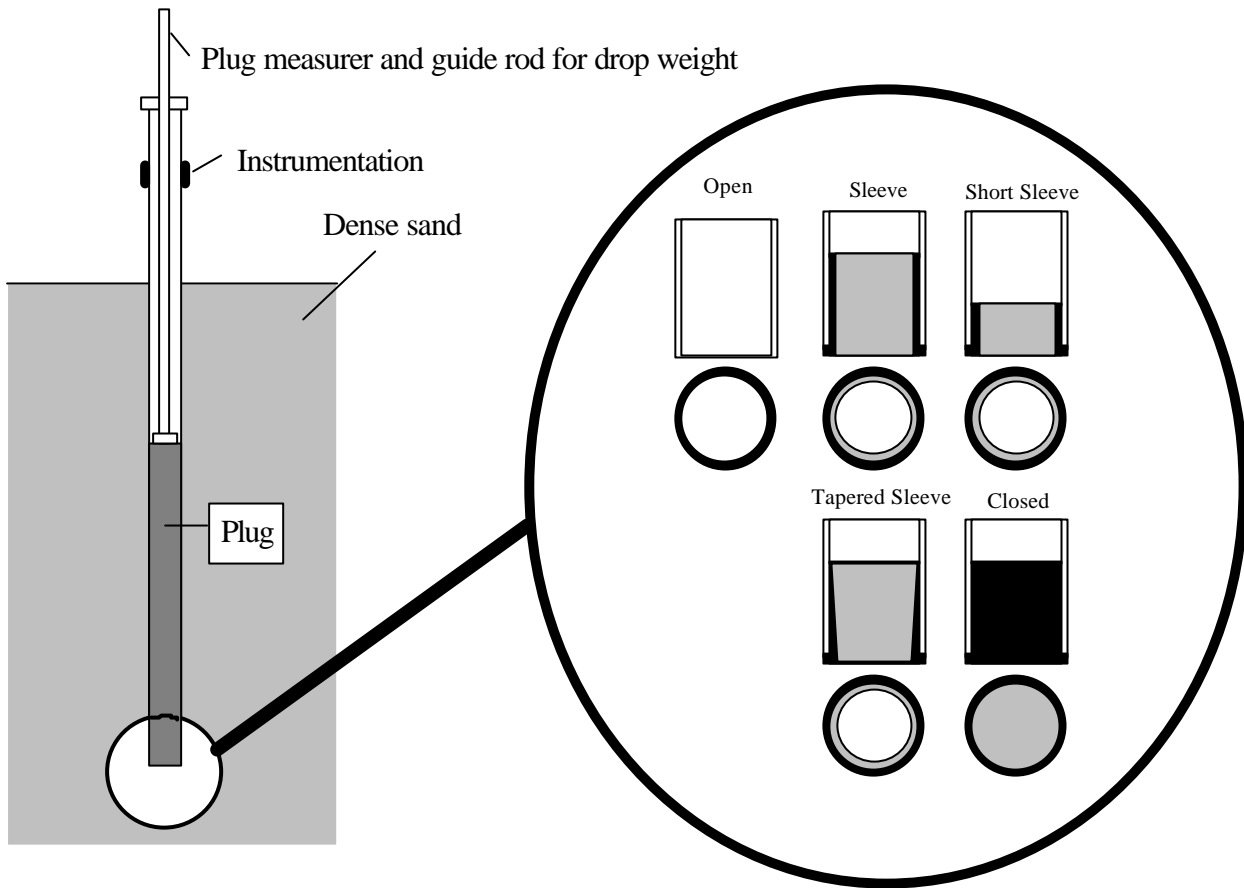


Figure 1 - Different end conditions imposed on the pile.

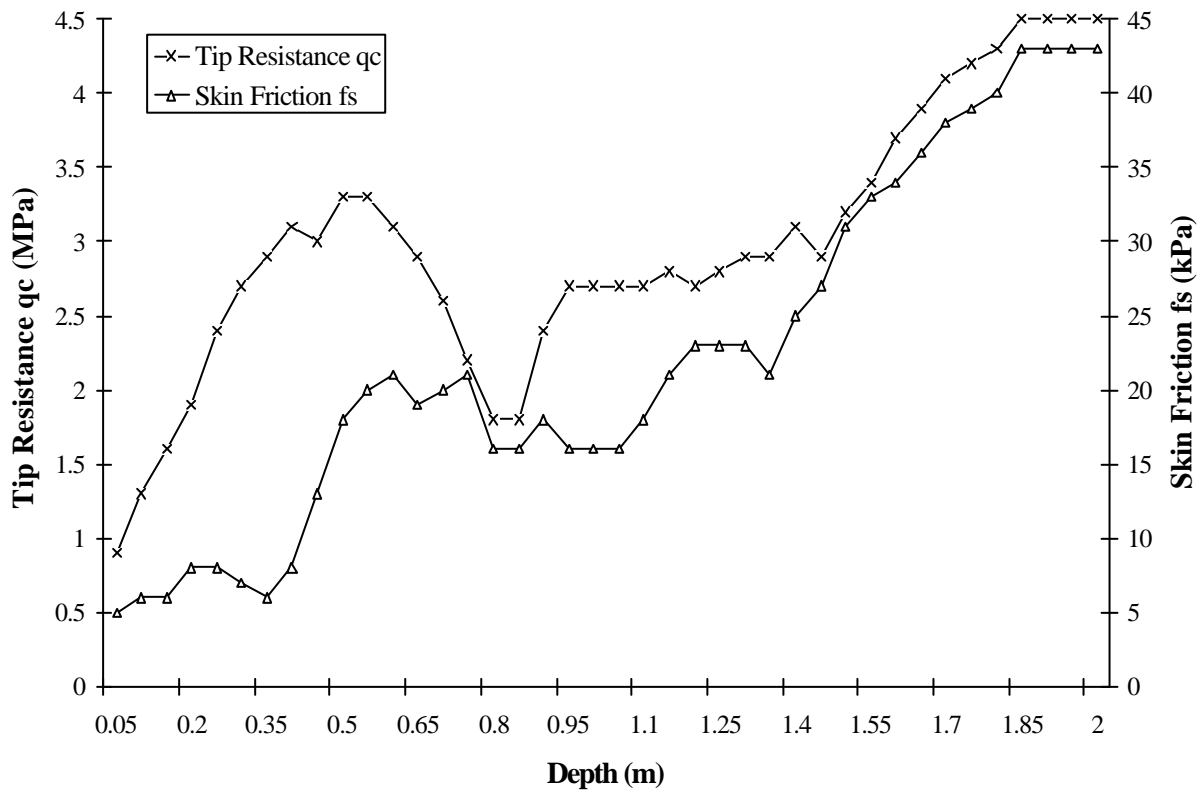


Figure 2 - Cone penetrometer results for the site at Shenton Park conducted in July 1993.

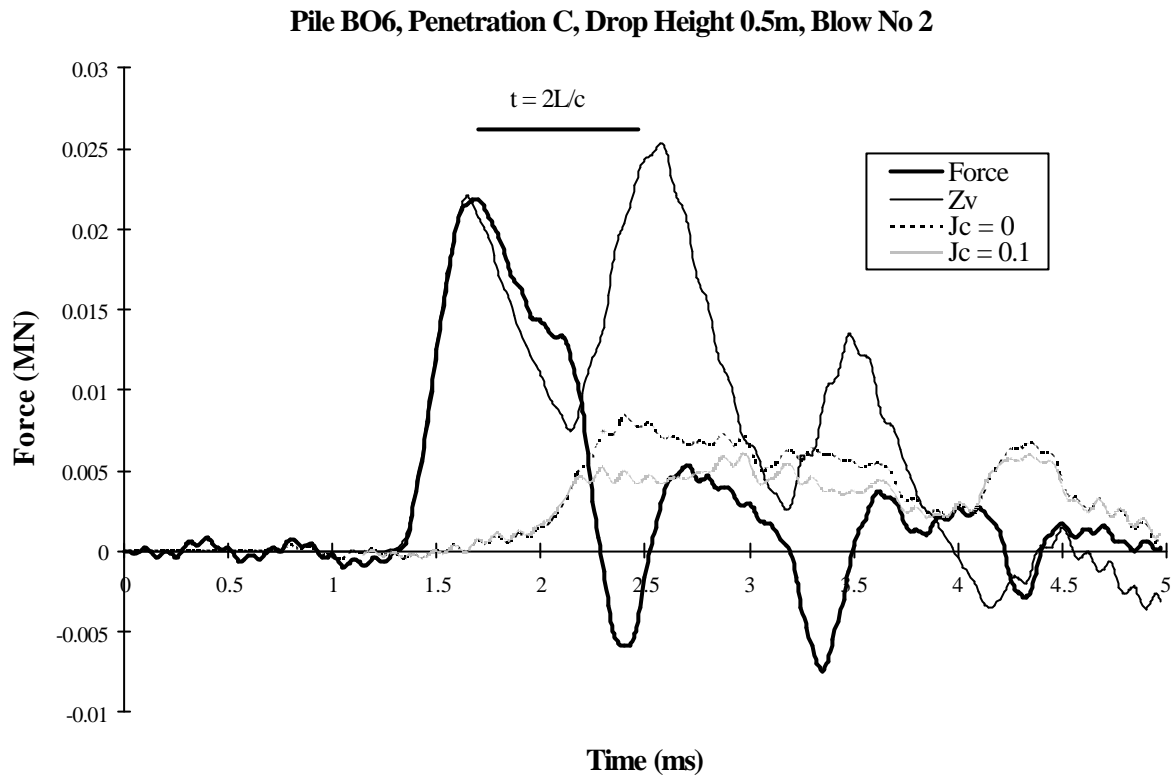


Figure 3 - Stress waves generated from the impact of the drop weight on the pile BO6 (including the calculated Case capacity).

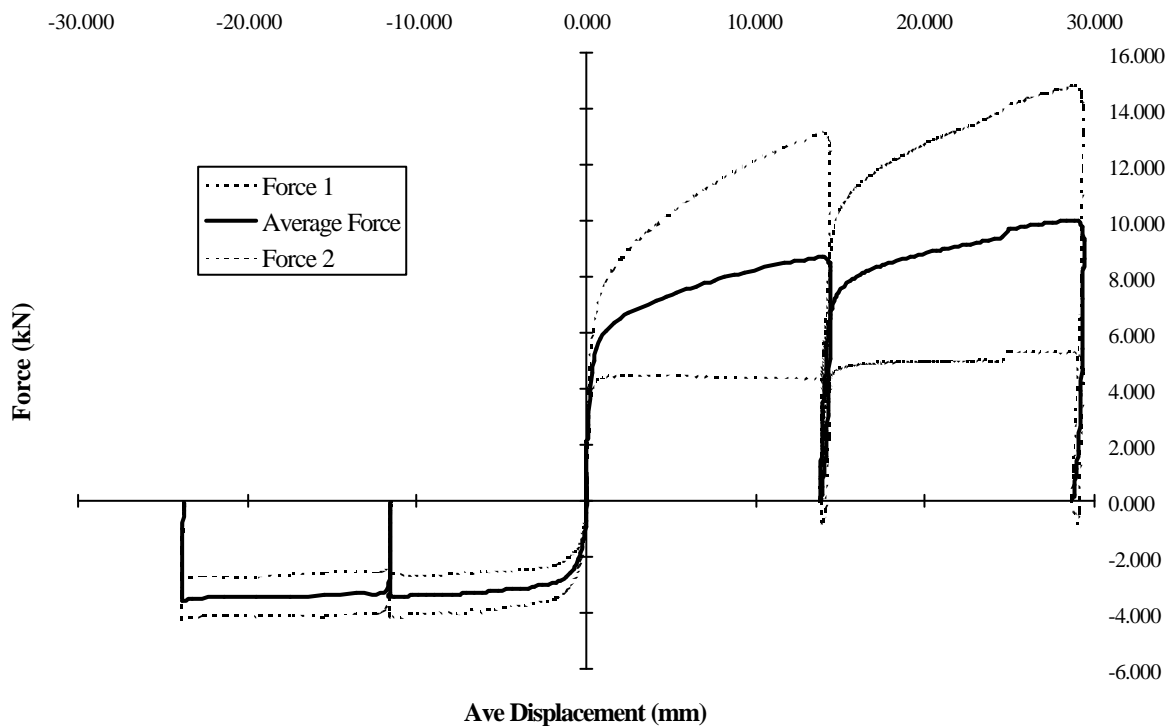


Figure 4 - Load displacement curve for the pile BO6.

Figure 5 - A typical stress wave fit produced in Impact.

Typical Impact Results	
Soil Resistance <ul style="list-style-type: none"> • External - 3.82 kN • Internal - 3.17 kN 	Shear Modulus <ul style="list-style-type: none"> • $G = 7.4z$ Mpa where z is depth in m.
Base Capacity <ul style="list-style-type: none"> • Annulus - 0.45 kN • Soil Plug - 3.24 kN 	Displacement Details <ul style="list-style-type: none"> • Set / Blow - 2.76 mm • Temporary Compression - 0.16 mm
Capacity <ul style="list-style-type: none"> • Plugged - 7.45 kN • Unplugged - 7.52 kN 	Energy Input <ul style="list-style-type: none"> • E_{in} - 0.0208 kJ
	Driving Formula Comparison <ul style="list-style-type: none"> • $R = 7.32$ kN

Figure 6 - Typical output from an Impact analysis.

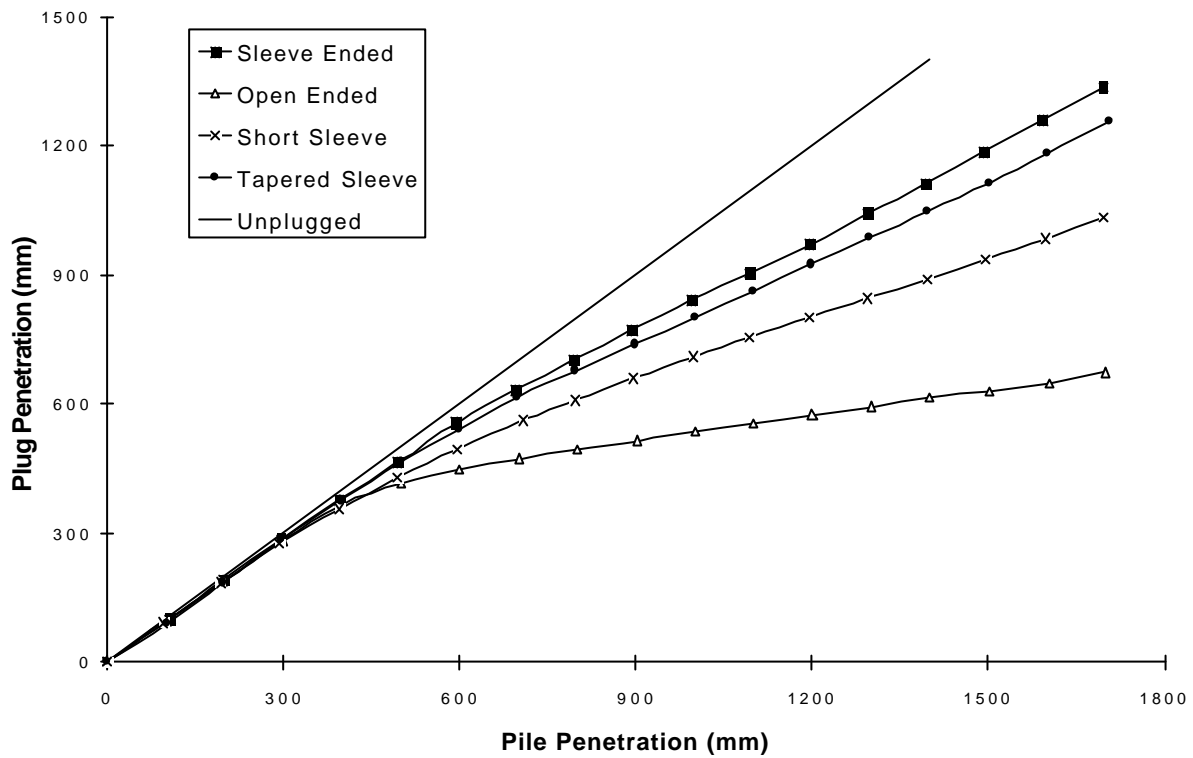


Figure 7 - Plug penetration versus pile penetration for the different pile types.

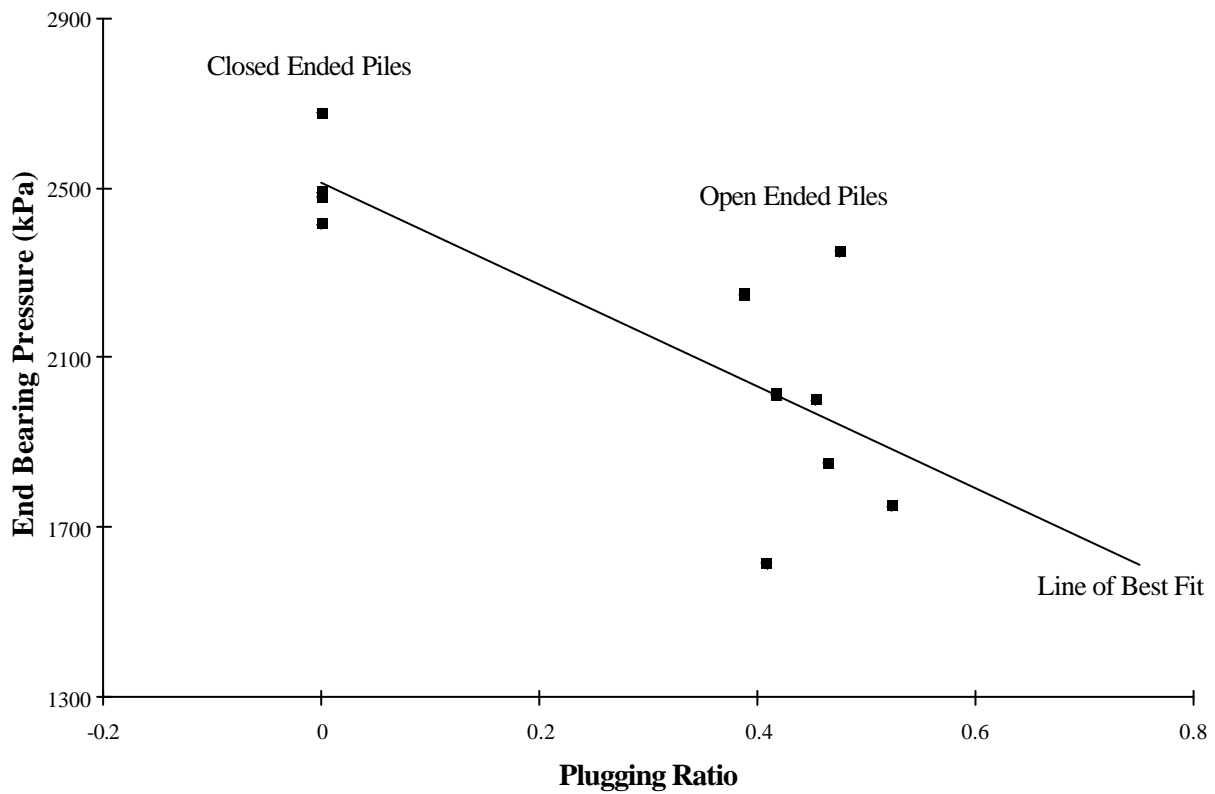


Figure 8 - End bearing pressure varying with the degree of plugging ratio.

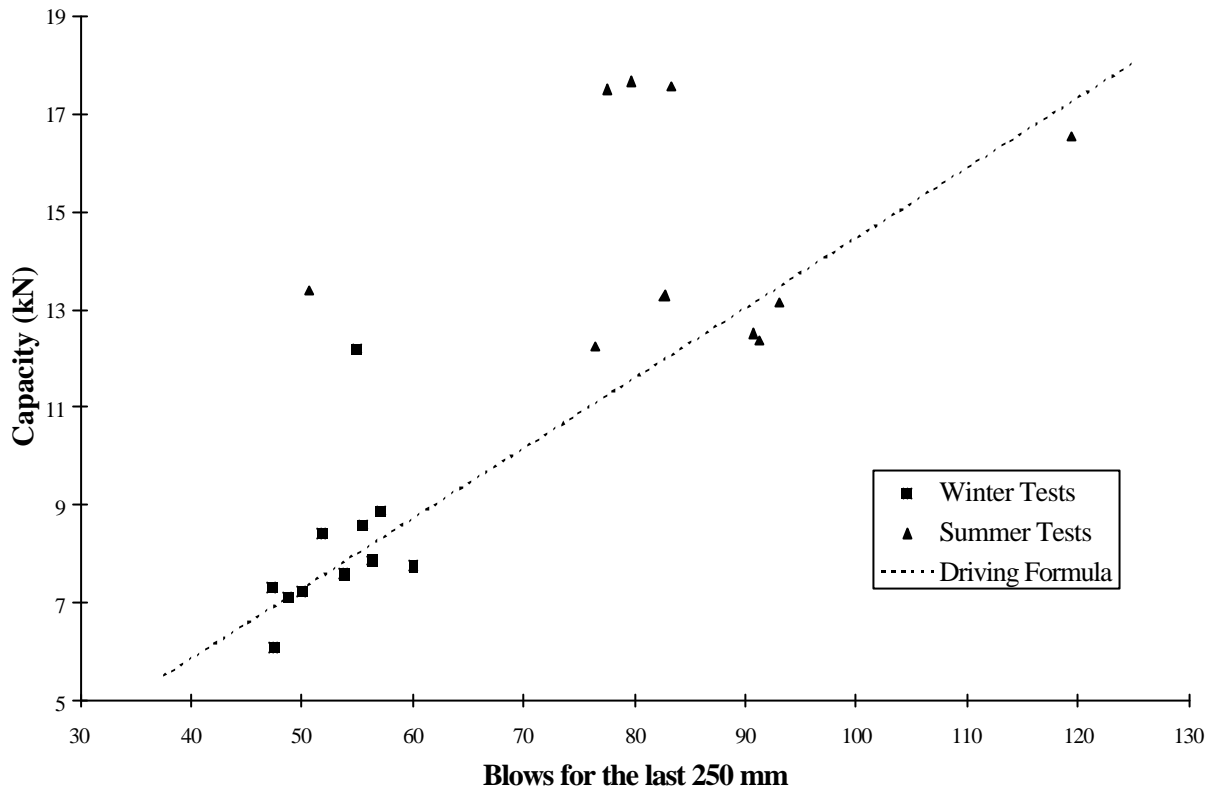


Figure 9 - The capacity versus the blow rate with a driving formula comparison.

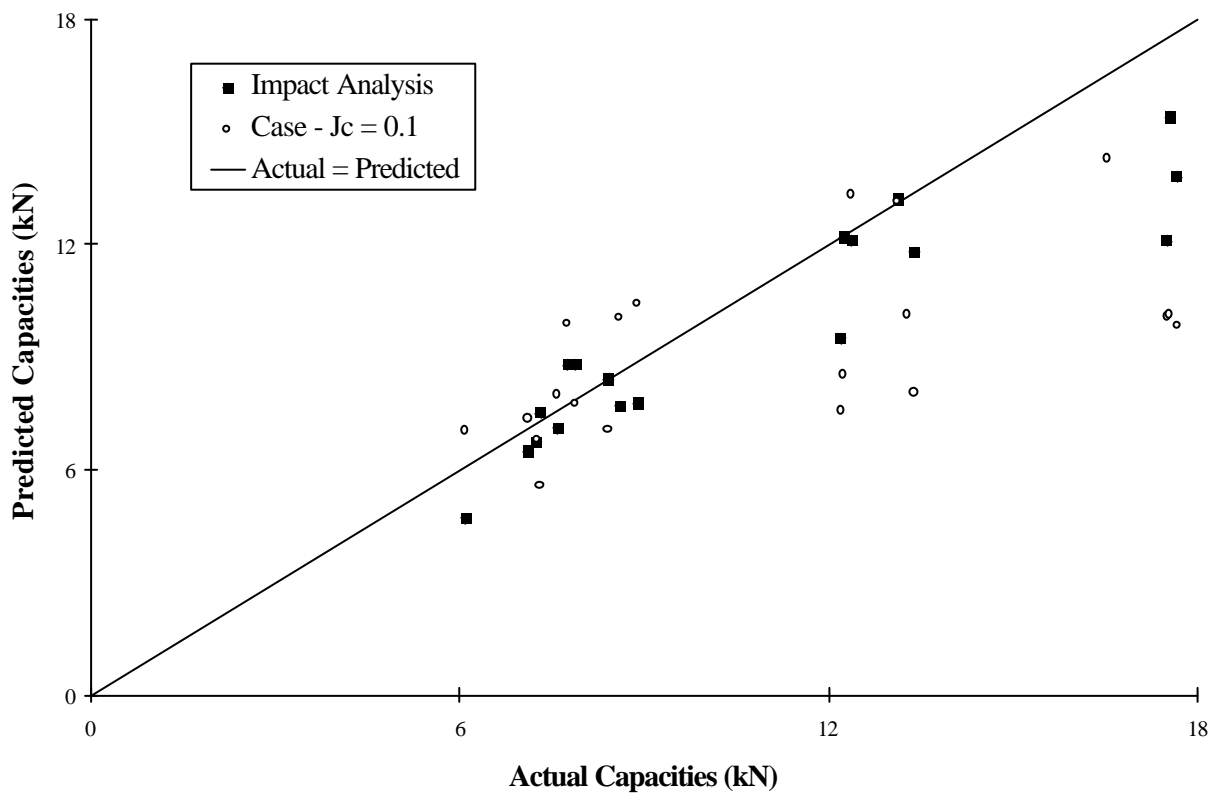


Figure 10 - The accuracy of predictions from dynamic measurements of axial capacity.